Transmission Switching, Demand Response and Energy Storage Systems in an Innovative Integrated Scheme for Managing the Uncertainty of Wind Power Generation

Jamshid Aghaei[a], Ahmad Nikoobakht[b], Mohammad Mardaneh[a],

Miadreza Shafie-khah[c], and João P. S. Catalão[c,d,e,*]

[a] *Department of Electrical and Electronics Engineering, Shiraz University of Technology, Shiraz, Iran*

[b] *Department of Elect & Control Engineering, Higher Education Center of Eghlid, Eghlid, Iran*

[c] *C-MAST, University of Beira Interior, Covilhã 6201-001, Portugal*

[d] *INESC TEC and the Faculty of Engineering of the University of Porto, Porto 4200-465, Portugal*

[e] *INESC-ID, Instituto Superior Técnico, University of Lisbon, Lisbon 1049-001, Portugal*

Abstract

This paper addresses the stochastic security constrained unit commitment (SSCUC) problem with flexibility resources for managing the uncertainty of wind power generation (WPG). Departing from the traditional flexibility resources such as the thermal units with fast up/down spinning reserves and transmission switching (TS), this paper explores also the use of demand response (DR) and energy storage (ES) systems in an innovative integrated scheme. The proposed scheme utilizes a stochastic optimization framework to coordinate the flexibility resources dealing with the uncertainty of WPGs and equipment failures. The stochastic optimization model is formulated as a mixed-integer linear programming (MIP), and this problem is large and computationally complex even for medium sized systems. Accordingly, we present a novel accelerating decomposition technique aimed at solving this problem and reducing the number of iterations and CPU time. Numerical simulation results on the modified 6-bus system and on large-scale power systems, i.e. IEEE 118 and 300-bus systems, clearly demonstrate the benefits of applying flexibility resources for uncertainty management and the efficacy of the proposed solution strategy for large-scale systems.

Keywords: Demand response; energy storage; wind power generation; transmission switching; uncertainty.

* Corresponding author at INESC TEC and the Faculty of Engineering of the University of Porto, Porto 4200-465, Portugal

Nomenclature

A. Indices and Sets

$(\cdot)^s$	Related to scenario *s*.
g, w, e	Index for units, wind units and storage, respectively.
$g(n) / w(n)$	Set of units/winds connected to the bus *n*.
$e(n)$	Set of storages connected to the bus *n*.
i, j	Energy blocks offered by (unit)/(load).
n	Bus index.
k, b	Transmission line index.
t	Time periods indices.
$k(n,.) / k(.,n)$	Set of line with n as the "to"/ "from" bus.
$\wedge$	Given variables/parameters.

B. Constants

P_g^{max} / P_g^{min}	Max/min capacity of unit *g*.
$X_{(\cdot),t-1}^{on} / X_{(\cdot),t-1}^{off}$	ON/OFF time of a demand at time *t*-1.
$DT_{(\cdot)} / UT_{(\cdot)}$	Minimum ON/OFF time of a demand.
$UL_k^{(\cdot)} / UG_g^{(\cdot)}$	Simulated (line *k*)/ (unit *g*) outage status.
P_k^{max}	Maximum power flow of line *k*.
$P_{w,(\cdot)}^{(\cdot)}$	Forecasted wind power output of unit *w*.
π_s	Probability of scenario *s*.
M	Separative factor; a large positive number.
B_k	Admittance of line *k*.
$\lambda_{i,g,(.)}^{G}$	Marginal cost of the *i*th block of energy offer by unit *g*.
$\lambda_{j,n,(.)}^{D}$	Marginal benefit of the *j*th block of energy bid by demand *n*.
C_n^{up} / C_n^{dn}	Cost of up/down spinning reserve of load *n*.
C_g^{up} / C_g^{dn}	Cost of up/down spinning reserve of unit *g*.

$DR_{(\cdot)}^{max}$ / $DR_{(\cdot)}^{min}$ Max/min curtailed demand.

$DE_{(\cdot)}$ Fixed hourly demand.

ΔD_n Pick-up or drop-off rate of demand *n*.

$E_{(\cdot)}^{max}$ Maximum energy change of a demand in the scheduling horizon.

$D_{(\cdot),t}^{max}$ Maximum hourly load.

MSR_g^{up} / MSR_g^{dn} Maximum up/down SR limits of unit *g*.

$SR_n^{up,max}$ / $SR_n^{dn,max}$ Maximum up/down SR limits of demand *n*.

$\overline{E}_e$ / $\underline{E}_e$ Max /Min state of storage *e*.

ρ_n / ρ_w Value of (lost load)/(wind power spillage).

$\overline{P}_e^c$ / $\underline{P}_e^c$ Max /min charge of storage *e*.

$\overline{P}_e^d$ / $\underline{P}_e^d$ Max /min discharge of storage *e*.

$\alpha_e^{c/d}$ Charge/discharge efficiency of ES unit.

C. Variables

$P_{g,(\cdot)}^{(\cdot)}$ / $P_{e,(\cdot)}^{(\cdot)}$ Power generation of (unit *g*)/(energy storage *e*).

$SR_{n,(\cdot)}^{up}$ / $SR_{n,(\cdot)}^{dn}$ Up/down spinning reserve of demand *n*.

$SR_{g,(\cdot)}^{up}$ / $SR_{g,(\cdot)}^{dn}$ Up/down spinning reserve of unit *g*.

$SU_{(\cdot)}$ / $SD_{(\cdot)}$ Startup/shutdown cost of a unit.

$MP_{1,(\cdot)}^{(\cdot)}$ / $MP_{2,(\cdot)}^{(\cdot)}$ Slack variables.

$WS_{(\cdot)}^{(\cdot)}$ / $LS_{(\cdot)}^{(\cdot)}$ (Wind power spillage)/(load shedding).

$\Delta P_{i,(\cdot)}^{(\cdot)}$ / $\Delta d_{j,(\cdot)}^{(\cdot)}$ Corrective dispatch capability of a unit/ demand at segment (*i*th)/(*j*th).

$\Delta R_{g,(\cdot)}^{(\cdot)}$ Reserve deployed by unit *g*.

$\Delta D_{n,(\cdot)}^{(\cdot)}$ Reserve deployed by load *n*.

$DR_{(\cdot)}$ / $D_{(\cdot)}^{(\cdot)}$ (Demand Response)/(hourly demand).

$W_{(\cdot)}^{(\cdot)}$ Objective function amount of the sub-problem.

$p_{i,(\cdot)}$ / $d_{j,(\cdot)}$ A (unit output)/(demand bid) at segment *i*/*j*. limited to $p_{i,g}^{max}$ / $d_{j,n}^{max}$.

$\Delta r_{i,(\cdot)}^{(\cdot)} / \Delta d_{j,(\cdot)}^{(\cdot)}$ Corrective dispatch capability of a unit/ demand at segment (ith)/(jth).

$P_{k,(\cdot)}^{(\cdot)}$ Power flow of line k.

$\theta_{k,(\cdot)}^{(\cdot)}$ Phase angle of line k.

$z_{(\cdot)} / u_{(\cdot)}$ Binary variable for state of (line k) /(unit g).

$u_{n,(\cdot)}$ Binary variable for demand n

$C_{e,(\cdot)}^{(\cdot)}$ State of charge of storage e , in %.

$\lambda_{(\cdot)}^{(\cdot)}, \mu_{(\cdot)}^{(\cdot)}, \eta_{(\cdot)}^{(\cdot)}, \vartheta_{(\cdot)}^{(\cdot)}$
$\psi_{(\cdot)}^{(\cdot)}, \xi_{(\cdot)}^{(\cdot)}, \gamma_{(\cdot)}^{(\cdot)}, \zeta_{(\cdot)}^{(\cdot)}$ Dual variables.

D. Abbreviations

BD Bender's decomposition.

DR Demand response.

DS Demand side.

DSR Demand side reserve.

ES Energy storage.

MIP mixed-integer linear programming.

NS Network side.

PSS Proposed solution strategy.

RER Renewable energy resource.

RMSE Root mean square error.

SA Storage Availability.

SS Supply side.

SSCUC Stochastic security constrained unit commitment.

SSR Supply side reserve.

TS Transmission switching.

WFE Wind forecast error.

WPG Wind power generation.

WPS Wind power spillage.

WSFE Wind speed forecast error.

I. Introduction

A. Motivation and Approach

One characteristic that sources of variable renewable generation such as wind, tidal, wave, solar, and run-of-river hydro have in common is having an output governed by atmospheric conditions. Especially, the wind power generation (WPG) may consequently be difficult to predict over some time scales [1]. Accordingly, the increasing penetration of WPG in recent years, a significant amount of wind power spillage (WPS) exists in practice. On the other hand, significant uncertainty and variability of high penetration of WPGs over shorter time scales can be problematic in power system operation.

One of the serious issues is how to keep increasing wind power penetration without endangering network reliability and security. Power system conditions will be more in danger when the uncertainty of high penetration of WPGs and equipment failures occurs simultaneously. In order to integrate the large penetrations of WPG without compromising the system security, more flexibility services are required to cope with the forecasted and expected changes in generation and system equipment failures.

Hence, the flexibility services provided by:

– *Supply side* (*SS*): Flexibility from the SS can be provided by up/down ramping capability or up/down-spinning reserve provided by this side (SSR).

– *Storage Availability* (*SA*): Storage units allow shifting the demand in time by storing electrical energy at the off-peak with low prices and high WPG periods and injecting it during peak hours with high prices and low WPG periods.

– *Demand side* (*DS*): The hourly DR can contribute to system flexibility through a number of actions, by lowering/increasing the peak/valley demand periods and shifting energy from high demand and low WPG to low demand and high WPG periods. In addition, the DS flexibility can be fully utilized by up/down spinning reserve (DSR). Indeed, it contributes to lower the stress on highly inflexible base-loaded units (e.g., nuclear power plants) to reduce their generation levels.

– *Network side* (*NS*): The most common reasons for curtailment are insufficient transmission capacity local congestion, and excessive supply during off-peak periods. Network reconfiguration, using TS action, is the capability of the network to mitigate the congestion and distribute energy and reserve throughout the network in real-time and increase the utilization of wind power under uncertainty.

The term *flexibility* describes the ability of a power system to cope with variability and uncertainty while maintaining a satisfactory level of reliability at a reasonable cost, over different time horizons. This definition interprets flexibility from both technical and economic points of view. Technically, flexibility is required to cope with uncertainties and

fluctuations in both generation and grid side. Economically, providing flexibility results in additional cost and this cost should be constrained within a reasonable range.

This paper proposes a stochastic SCUC model (SSCUC) which considers *cooperation of simultaneous flexibility resource options* including the hourly economic and emergency DR program, network reconfiguration by the TS action, ES system, up/down- spinning reserve provided by dispatchable units for minimizing the daily expected operation cost (EOC) under uncertainty condition. The day-ahead forecast errors of hourly WPG and random outages of generators and transmission lines are treated as uncertainties in this study. The solution to the original stochastic SCUC problem with the DR program in each load bus, the TS action, for all transmission lines, the ES system, and thermal generation flexibility, *simultaneously*, in such cases would be an intractable task without effective solution strategy, especially for large-scale systems. For this reason, in this paper, an accelerating decomposition technique is proposed based on combining the Benders' decomposition and a novel heuristic technique for pre-screen lines for the TS action to solve stochastic SCUC problem through the innovative integrated allocation of flexibility resources in the large-scale systems under uncertainty.

B. Literature Review

Conventional power plants are used today in power systems to supply almost all the flexibility needed. The flexibility attributes of a conventional generator may include its ramp rate, minimum stable output, and minimum start, stop, up, and down times. While flexibility resources are commonly found in the SS, there is also the possibility of harvesting flexibility from NS (or TS action). Recent advances in information and communication technologies, together with the large-scale rollout of smart grids, have created a new window of opportunity to make better use of NS to increase flexibility [2].

One of the effective approaches to reduce the system congestion and increase the amount of the ramping capability in the power systems is to implement the TS action. Also, the TS action is a straightforward way for the NS flexibility to make better use of the existing network and improve system performance [3].

The TS action can enhance the deliverability of reserves and reroute the network power flow [4]. Also, the TS action is shown to be a viable solution for handling high penetration of WPGs, which is also significantly cheaper than many alternatives [5]. Thus, the TS action is a low cost power flow control technology that would reduce the operational costs, improve system reliability, and enhance integration of intermittent WPGs [3].

One of the concerns in performing the TS action in particular is frequently lines switching in successive hours, it should be noted that frequently lines switching can create undesirable effects on the security and reliability of power systems and may require new investments in the automation and control systems. As a result, the topology of the power network is not allowed to be changed too frequently [6] and [7]. For this reason, to maintain a secure system against to change network topology, the actions considered in particular for TS action are as follows:

1) – the power system operator pre-screened a priority list for switchable line candidates, after determining switchable line candidates, the network security constraints are checked for switching action of these lines, and if the network security constraints are satisfied, these lines, for switching action, are suggested [8].

2) - One of the concerns in performing the TS action in sequential time is the possibility of high standing phase angle (SPA) difference through a switchable line candidate. If a switchable line candidate causes a loop closure, quick changes may be necessary in the generation redispatch, which could otherwise impact the rotor of a unit generation. An extreme torque may be induced in the rotor of a unit generation that can lead to equipment failure and unit generation weakness [9] ,[10]. This may happen to any unit generations irrespective of their connectivity to the closed a switchable line candidate. Consequently, it is required to bound the SPA difference to safeguard the rotor of a generator. Commonly a generation redispatch upon line closures would bring the SPAs back to the safe region. Different approaches are proposed to obtain the minimum generation redispatch needed to achieve desired SPAs in a wise time [6] and [11]. This issue which is inevitable in restoration practices may also occur in the normal operation of power systems once attempting to reclose a single line that is a part of a transmission loop [7] and [11]. The SPA difference bound of switchable lines are approximately determined based on the voltage levels. The practical settings are 60◦ for 115 kV, 40◦ for 230 kV and 20◦ for 500 kV power systems [10].

In [12] a stochastic SCUC problem under the WPG uncertainty is presented, and some flexibility resources such as DS and SA are considered. This reference discusses a potential problem formulation, but numerical results are not reported.

In [13] and [14] a stochastic day-ahead scheduling of electric power systems with flexibility resources is proposed to manage the variability of renewable energy sources. The flexibility resources include thermal units with up/down ramping capability, ES system, and hourly DR.

The demand response (DR) program facilitated by smart grid technologies would adjust electricity consumption patterns in which customers would benefit from cheaper electricity during off-peak hours as customers play a more active role in power system operations [15]. The most efficient power market dynamics would be achieved when incorporating both the flexible generation and demand side management [16].

However, with the recent increase in hourly DR [15], [13] and [17] and, flexible demands can contribute to integrate increasing amounts of WEPs.

The contribution of demands in providing flexibility from the system operator point of view is discussed in [17, 18].

Ref. [18] focuses on the utilization of DR and ES system that would provide ISOs more flexible options for scheduling the available energy resources in a day-ahead scheduling. However, the issue of uncertainty management with DR and ES is not addressed.

The main disadvantage of these references (i.e., [17] and [18]), is that an efficient and powerful solution strategy is not presented to solve our proposed problem with a large number of scenarios, for this reason, the TS action cannot be considered in these stochastic problems and our proposed problems might be intractable due to the increased size of variables and constraints in the large-scale systems with a large number of scenarios.

Today, various combinations of hydro, as an SA in power system, and thermal generation are used to manage variability; these operate as a portfolio to meet demand. For example, in [19], demonstrates that the hourly coordination of the WPG units with pumped-storage hydro generation can mitigate the variability of WPG and increase its dispatchability.

In addition, most researchers agree that ES system is cardinal to a renewable energy future. The ES system will not only help to support shortfalls between supply and demand, but also provide flexibility in the operation and management of the WEPs uncertainty [9] and [18]. The ES systems provides two-fold advantage in power systems with WEPs, firstly it reduces the ramp up/down stress on conventional thermal units induced by WEPs and secondly it reduces the up-/down-ramping requirements [18].

In many ways, storage seems like an ideal flexibility resources. It is quick to respond, can increase as well as decrease net demand, and in the case of battery storage can be deployed close to the load in a modular fashion [12]. Providing power system flexibility with storage can generally be thought of as providing energy, power, or a combination of both.

The role of the ES system in the integration of RERs was addressed in [18]. The integration of ES system in power systems was investigated in [18] and major issues for the integration of RERs were discussed. References [9] studied the integration of storage for mitigating the effect of hourly wind energy variability on power systems.

Moreover, in this reference [20] the BD technique is used to decompose the original large-scale stochastic SCUC problem, with a few scenarios, into one tractable master MIP problem and several linear programming sub-problems.

In [13] and [14] a stochastic SCUC problem is presented in which the wind, load forecast errors and units contingencies are considered. In these references, the effect of hourly DR is considered as a means of mitigating transmission violations when uncertainties are considered.

The solution strategy proposed in these references [13] and [14] is not efficient for the large-scale stochastic SCUC problems with a large number of scenarios, due to the master problem of BD technique in these references include both first- and second-stage variables. In addition, in this reference, the TS action has been not considered.

In [3], [10] and [21] to improve the efficiency of the transmission network and enhance the utilization of WPG (reduce WPS), the TS action has been applied to accommodate higher utilization of WPG and reduce the daily operation cost. In these references, the stochastic problem is solved based on the general BD method.

The general BD method proposed in these references [3], [10] and [21] is a good solution strategy for one flexibility resource, i.e., the TS action with a few number of switchable lines, but by adding other flexibility resources, (i.e., DR and/or ES unit and considered large number of switchable lines), to its stochastic problem, the performance of solution strategy is significantly reduced and the problem might be intractable, due to increased size of variables and constraints in master problem for each benders iteration.

In addition, the main disadvantage of the BD method proposed in these references to solve our problem is that it may require a very large number of iterations to achieve convergence, which will increase the computation time, significantly.

Accordingly, it is not efficient for the large-scale stochastic SCUC problem with a large number of scenarios and switchable lines.

As shown in Table I, except current paper, no reference in the literature, which was published in recent years, simultaneously considers entire flexibility resource options in stochastic SCUC models. The main reasons are the computational time and considerable difficulties of solving our proposed model for a large-scale system with a large number of scenarios and switchable lines. Moreover, the references brought in Table I, are not presented an effective solution strategy to solve our model, which is presented in this paper.

C. Contributions

The novelties of this work are threefold:

- Managing the uncertainty of high penetration of WPGs using *simultaneously coordinated* operation of flexibility resources including the up/down-spinning reserves provided by dispatchable units and demand side (i.e., SSR/DSR), ES units, hourly DR and TS action.
- Developing an accelerating and effective solution strategy based on combining the Benders' decomposition and a novel heuristic technique for pre-screen lines for the TS action to solve the stochastic SCUC problem through the innovative integrated allocation of flexibility resource options in a large-scale system and a large number of switchable lines for the TS action. Accordingly, the proposed solution approach is effective even if hundreds of scenarios are considered to describe uncertain data.
- Comparing the *computation time and optimal solution* of our accelerating decomposition strategy with other available solution strategies in existing references, to solve our proposed problem for a large-scale system, i.e., IEEE-300 bus system.

It should be noted that, the application and operation of flexibility resources, with different models, can be individually implemented for different problems with different features, existing in available references [3], [16], [17] and [22]. But, in the application of *simultaneously coordinated* operation of flexibility resources in an SSCUC problem,

it is essential to know "*How is it solved in a reasonable time*?". Answering to this question makes different our proposed problem from others which are mentioned in the above literature review. Accordingly, the proposed novel accelerating decomposition technique to solve our proposed problem, with all kinds of flexibility resources, is not a trivial task and is the very complicated task.

To the best of the authors' knowledge, no reference has provided the stochastic SCUC formulation with four flexibility resources (i.e., NS, DS, SA and SS) in the presence of WPG uncertainty and equipment failures, making it possible the use of accelerating decomposition strategy.

D. Paper Organization

The remainder of this paper is organized as follows: Modelling of system uncertainties is addressed in Section II. The problem formulation is addressed in Section III. Section IV proposes the solution methodology. Section V presents the results obtained from simulations of the modified 6-bus system and the IEEE 118-bus large-scale system. Concluding remarks are drawn in Section VI.

Table I: Taxonomy of the flexible resource options proposed in this paper.

Ref	Year	NS	DS	SA	SS	DSR	SSR	Stochastic	
								Wind	Unit/Line
[12]	2013	N	Y	Y	Y	N	Y	Y	Y
[13]	2015	N	Y	Y	Y	N	N	Y	Y
[23]	2013	N	Y	Y	Y	N	N	Y	Y
[18]	2014	N	Y	Y	Y	N	N	N	N
[24]	2013	N	N	Y	Y	N	Y	Y	Y
[25]	2013	N	Y	N	Y	Y	Y	Y	Y
[10]	2015	Y	N	N	Y	N	Y	Y	N
[26]	2015	Y	N	N	Y	N	N	Y	N
[27]	2013	N	N	N	Y	N	Y	Y	Y
[28]	2015	N	Y	Y	Y	N	Y	Y	Y
CP	-	Y	Y	Y	Y	Y	Y	Y	Y

Y/N denotes that the subject is/is not considered, CP: current paper

II. Modelling of System Uncertainties

The proposed stochastic SCUC model with flexible resources utilizes MCS for representing power system uncertainties, which include day-ahead forecast errors of hourly WPG and random outages of thermal units /transmission lines. The MCS parameters are forced outage rates of power system components and Weibull distribution functions of forecast errors for hourly wind speed. The proposed SSCUC problem includes the following uncertainties:

A. Forecast Errors of Hourly WPG

In this study, the just WPG has been considered. The WPG is characterized by measured speed data and parameters for a wind farm. The wind farm related parameters include the geographic information (a low number of weather stations are used to estimate wind speed and direction over a wide geographical area) and the temperature information (nominal ambient temperature or a time series of ambient temperature are used to estimate wind speed). The wind speed forecast error (WSFE) is described by the auto-regressive moving average (ARMA) [29]. Since the autocorrelation factor of the wind speed time series would decrease dramatically as the time lag increases, the hourly WSFE is represented by a lower order ARMA (1, 1). The ARMA constants are acquired by minimizing the root mean square error (RMSE) between the simulated ARMA time series and the measured wind speed data [29]. In this study, the simulated ARMA time series are used, which constant parameters and its formulation are given in reference [13].

Also, synthetized wind speed time series is used to denote the time series for the hourly WSFE [30]. The forecasted wind speed time series is obtained by implementing the Markov process transition probability matrix (TPM), which is characterized by probability distribution parameters of wind speed time series [30]. Using the Weibull distribution function (WDF) and the autocorrelation factor, the TPM is procured by composing an initial probability vector, a weighting matrix, and a normalizing vector [30]. Once the TPM is constructed, the wind speed time series is synthesized using the Markov chain method [30]. To include diurnal fluctuations, wind speed time series data is multiplied by the diurnal pattern, i.e., sinusoidal scale factors. The peak value in this pattern indicates the ratio of the maximum wind speed to the daily average wind speed [30]. The hourly WPG is then obtained using the hourly wind speed and the power curve of wind turbines.

B. Monte Carlo Simulation

To deal with the uncertainty of wind speed, many works have been reported in the literatures. Monte Carlo simulation combined with simple random sampling is one of the most popular methods [31]. If the sample size is large enough, people will get the simulation results with high accuracy. However, it also brings about heavy computational burden for the need of a large number of repeated calculations. This paper applies a Latin hypercube sampling (LHS) method, which is proposed by Mckay [32], to handle the uncertainties. The LHS method is divided into two main steps including sampling and permutation. In this paper, the Cholesky decomposition is applied [33], [34]. After the LHS method is applied, a scenario reduction is needed to obtain smaller number of scenarios that can represent reasonably good approximations [33].

In order to improve the efficiency of the MCS simulation, a low discrepancy method, Latin Hypercube Sampling (LHS), is utilized to generate evenly distributed random samples with smaller variance [35]. In addition, outages of thermal units and transmission lines are simulated based on forced outage rates (FOR) which determine the hourly

availability of thermal units and transmission lines. Scenario reduction techniques are used to find a tradeoff between the computation speed and the accuracy [30].

In addition, computational requirements for solving stochastic optimization models depend on the number of scenarios. Therefore, an effective scenario reduction technique could be very essential for solving large-scale systems. The reduction method is a scenario-based approximation with a smaller number of scenarios and a reasonably worthy approximation of original system. So, we determine a subset of scenarios and a probability measure based on this subset that is the closest to the initial probability distribution in terms of probability metrics. Our scenario reduction technique would control the goodness-of-fit of approximation by measuring a distance of probability distributions as a probability metric. Efficient algorithms based on backward and fast forward methods are developed that determine optimal reduced measures. Simultaneous backward and fast forward reduction methods are briefly introduced here as follows [30].

The General Algebraic Modeling System (GAMS) is used in this study. GAMS provides a tool called SCENRED for scenario reduction and modelling random data processes. The backward reduction, fast forward reduction, and other methods for large scenario reductions are included in the SCENRED library [36]. These scenario reduction algorithms provided by SCENRED determine a scenario subset (of prescribed cardinality or accuracy) and assign optimal probabilities to the preserved scenarios [37] and [30].

III. Stochastic SCUC Formulation

Objective function: The objective function, expressed in (1), is to determine the first-stage unit commitment and second-stage hourly schedules for generating units (including SS spinning reserve), WPS, DR (including DS spinning reserve) and energy storages so as to maximize the total social welfare in the base case and all scenarios. Here, there is no cost term in the objective function (1) related to the operation of WPG units, because wind farms generally have low operation costs. The objective function (1) is the EOC which consists of six terms: (i) the energy cost block of the generating units minus the demand utility [13]; (ii) the startup/shutdown cost of the thermal units; (iii) the cost of up/down SR from demands named cost of demand side reserve (DSR); (iv) the cost of up/down spinning reserve (SR) from thermal units named cost of supply side reserve (SSR); (v) the cost related to the actual deployment of up/down SR by units and demands separately; and (vi) the cost of involuntary load shedding and WPS due to WPG variability. It is noted that the first stage in (1) involves the hourly WPG forecasts without considering any system equipment failure.

System and unit constraints: Limits on the generation of units with up/down SR is given in (2). Energy generation block (in the multiblock offer) of units and its limits are defined in (2) and (3), respectively. Also, the amounts of 10-min up/down SR which can be provided by each generating unit are limited by (4) and (5). Constraint (6) links between the base case and scenario variables of thermal units to enforce corrective actions by up/down SR, i.e., $\Delta R^{s}_{g,t}$. The deployed up/down SR of on-line units in the real-time for each scenario is determined by (7). In order to consider the

cost of SR deployment, the deployed SR from generating unit is decomposed into corresponding energy blocks in the multi-block offer. Also, in (7) decomposes the deployed SR of unit *g* into energy blocks [13], (i.e., $\Delta R^s_{g,t} = \sum_i \Delta r^s_{i,g,t}$). Constraint (8) enforces that the blocks of deployment of SR are subtracted (or added in case of up-SR) from the blocks of energy. Then, the cost of deployment of SR of unit *g* in scenario *s* can be represented as $\sum_i \lambda^G_{i,g,t} \cdot \Delta r^s_{i,g,t}$, which is included in the objective function (1). A percentage of the available WPG can be spilled to facilitate the power system operation. This is imposed by (9). Constraint (10) is the power balance equation. Also, constraint (11) is the TS formulation as presented in [2]. The *M* is necessarily a large number. In these constraints, once $z_{k,t}$=1 and $UL^s_k = 1$ line *k* is closed, and Kirchhoff's law is employed; and once $z_{k,t}$=0 and $UL^s_k = 0$, line *k* is open, so, Kirchhoff's law no longer can be employed, and the power flow of the line is zero. The maximum power flow of each line if that line is closed is defined by (12). The binary parameter UL^s_k forces the line's power flow to be zero within (12) once the line is the contingency; the use of UG^s_g in (6) and (7) forces a thermal unit's generation to be zero when the unit is the contingency.

$$Min \sum_t \left\{ \begin{array}{l} \overbrace{\sum_g \sum_i (\lambda^G_{i,g,t} \cdot p^0_{i,g,t}) - \sum_n \sum_j (\lambda^D_{j,n,t} \cdot d^0_{j,n,t})}^{\textbf{First-stage}} \\ + \sum_g (SU_{g,t} + SD_{g,t}) \\ + \sum_n (C^{up}_n \cdot SR^{up}_{n,t} + C^{dn}_n \cdot SR^{dn}_{n,t}) \\ + \sum_g (C^{up}_g \cdot SR^{up}_{g,t} + C^{dn}_g \cdot SR^{dn}_{g,t}) \\ \overbrace{+ \sum_s \pi_s \cdot \left[\begin{array}{l} \sum_g (\sum_i \lambda^G_{i,g,t} \cdot \Delta r^s_{i,g,t}) + \sum_n \sum_j (\lambda^D_{j,n,t} \cdot \Delta d^s_{j,n,t}) \\ + \sum_n \rho_n \cdot LS^s_{n,t} + \sum_w \rho_w \cdot WS^s_{w,t} \end{array} \right]}^{\textbf{Second-stage}} \end{array} \right\} \quad (1)$$

$$P^{min}_g u_{g,t} + SR^{dn}_{g,t} \le P^0_{g,t} = \sum_i p^0_{i,g,t} \le P^{max}_g u_{g,t} - SR^{up}_{g,t} \quad (2)$$

$$0 \le p^0_{i,g,t} \le p^{max}_{i,g} \quad (3)$$

$$0 \le SR^{up}_{g,t} \le u_{g,t} MSR^{up}_g \times 10\ min \quad (4)$$

$$0 \le SR^{dn}_{g,t} \le u_{g,t} MSR^{dn}_g \times 10\ min \quad (5)$$

$$P^s_{g,t} = P^0_{g,t} UG^s_g + \Delta R^s_{g,t} \quad (6)$$

$$-SR^{dn}_{g,t} UG^s_g \le \Delta R^s_{g,t} = \sum_i \Delta r^s_{i,g,t} \le SR^{up}_{g,t} UG^s_g \quad (7)$$

$$-p^0_{i,g,t} \le \Delta r^s_{i,g,t} \le p^{max}_{i,g} - p^0_{i,g,t} \quad (8)$$

$$0 \le WS^s_{w,t} \le P^s_{w,t} \quad (9)$$

$$\sum_{\forall g(n)} P_{g,t}^{s} + \sum_{\forall w(n)} (P_{w,t}^{s} - WS_{w,t}^{s}) + \sum_{\forall e(n)} P_{e,t}^{s} + \sum_{\forall k(.,n)} P_{k,t}^{s} - \sum_{\forall k(n,.)} P_{k,t}^{s} = D_{n,t}^{s} \tag{10}$$

$$B_k \theta_{k,t}^{s} - M(1 - z_{k,t} UL_k^{s}) \le P_{k,t}^{s} \le B_k \theta_{k,t}^{s} - M(1 - z_{k,t} UL_k^{s}) \tag{11}$$

$$-P_k^{max} z_{k,t} UL_k^{s} \le P_{k,t}^{s} \le P_k^{max} z_{k,t} UL_k^{s} \tag{12}$$

$$\sum_{j} d_{j,n,t} = DE_{n,t} - DR_{n,t} = D_{n,t}^{0} \tag{13}$$

$$0 \le d_{j,n,t} \le d_{j,n}^{max} \tag{14}$$

$$\begin{cases} u_{n,t} DR_{n,t}^{min} \le DR_{n,t} \le u_{n,t} DR_{n,t}^{max} \\ DR_{n,t} \ge DE_{n,t} - D_{n,t}^{max} \end{cases} \tag{15}$$

$$\left| DR_{n,t} - DR_{n,t-1} \right| \le \Delta D_n \tag{16}$$

$$(X_{n,t-1}^{on} - UT_n)(u_{n,t-1} - u_{n,t}) \ge 0 \tag{17}$$

$$(X_{n,t-1}^{off} - DT_n)(u_{n,t} - u_{n,t-1}) \ge 0 \tag{18}$$

$$0 \le \sum_{t} DR_{n,t} \le E_n^{max} \tag{19}$$

$$D_{n,t}^{s} = D_{n,t}^{0} + \Delta D_{n,t}^{s} - LS_{n,t}^{s} \tag{20}$$

$$-SR_{n,t}^{dn} \le \Delta D_{n,t}^{s} = \sum_{j} \Delta d_{j,n,t}^{s} \le SR_{n,t}^{up} \tag{21}$$

$$-d_{j,n,t} \le \Delta d_{j,n,t}^{s} \le d_{j,n}^{max} - d_{j,n,t} \tag{22}$$

$$0 \le SR_{n,t}^{up} \le u_{n,t} SR_n^{up,max} \tag{23}$$

$$0 \le SR_{n,t}^{dn} \le u_{n,t} SR_n^{dn,max} \tag{24}$$

$$0 \le LS_{n,t}^{s} \le D_{n,t}^{0} + \Delta D_{n,t}^{s} \tag{25}$$

$$P_{e,t}^{s} \in \left\{ 0, \left[-\overline{P}_e^{c}, -\underline{P}_e^{c} \right], \left[\underline{P}_e^{d}, \overline{P}_e^{d} \right] \right\} \tag{26}$$

$$C_{e,t}^{s} = C_{e,t-1}^{s} - \frac{\alpha_e^{c/d} \cdot P_{e,t}^{s}}{\overline{E}_e} \tag{27}$$

$$\frac{\underline{E}_e}{\overline{E}_e} \le C_{e,t}^{s} \le 1 \tag{28}$$

$$C_{e,0}^{s} = C_{e,24}^{s} = C_e^{0} \tag{29}$$

Hourly DR Constraints: The DR constraints in the stochastic SCUC are listed in (13)–(25). Considering multi-block offer for demand response, the relationship between demand block and the total demand is given in (13). The limit on each block is provided in (14). The responsive demand limit is defined in (15), where $DR_{d,t}^{0}$ is positive when the

demand is shifted out from time *t*, and is negative when the demand is shifted to time *t*, and zero when there is no demand shedding or shifting. The demand response rate is limited in (16) by the customer ramping ability for adjusting demands. In (17) and (18), minimum up and down time are the minimum number of successive periods that the demand would be supplied or shed. Constraint (19) enforces the limit on the acceptable demand changes through the daily scheduling in which the decreased demand at t will be shifted to other times if $E_d^{max} = 0$. The actual demand consumption with deployed up/down SR and involuntary demand shedding for each scenario is enforced by (20). The constraints on deployed up/down SR from demand side are enforced by (23)-(24). Similar to the constraints (4) and (5), the deployed SR from demands can be decomposed by (21) and (22). Then, the cost of deployment of SR of demand n in scenario s can be represented by $\sum_j \lambda_{j,n,t}^{D} \cdot \Delta d_{j,n,t}^{s}$, which is included in the objective function (1). Constraint (25) shows the maximum involuntary demand shedding of each demand in each scenario.

Energy storage constraints: The ES units constraints include output and input power limits, state of charge (SOC) dynamics, SOC limits, and limits on initial and final SOC, which are defined in (26)–(29), respectively. Equation (26) considers three states for ES units: 0 once the ES unit is not in operation; charging state, i.e., $\left[-\overline{P}_e^c, -\underline{P}_e^c\right]$; and discharging state $\left[\underline{P}_e^d, \overline{P}_e^d\right]$. The linear formulation of implementing this equation can be found in [14]. State of charge and discharge is determined by (27). Limits on ES unit capacity is given in (28). Constraint (29) suggests that the ES unit follows a daily cycle; that is, the SOC at the initial time (t = 0) is equal to that of the last period in the scheduling horizon (t = 24).

IV. Proposed accelerating decomposition technique

As shown in Fig.1, the proposed solution strategy has two parts, the first part related to the BD technique and the second part related to heuristic prescreening switchable lines in order to accelerate solving the stochastic SCUC problem with TS action. The detail of the proposed solution strategy is described below.

A. The first part (Bender's decomposition approach)

The proposed stochastic SCUC problem with flexibility resources (especially NS flexibility) in (1)–(29) is a large-scale, non-convex problem. The corresponding solution of our proposed problem for large-scale systems would be an intractable task without decomposition strategy. The benders' decomposition approach is implemented to decompose the original proposed stochastic SCUC problem with flexibility resources into one master problem and tractable first and second sub-problems. The formulation of Benders' master problem and sub-problem in detail are provided as follows:

Master Problem: The master problem corresponding to the original problem is formulated as (30)-(33) below. The objective function (30) corresponds to (1), where α represents the expected cost in real-time operation:

Objective function:

$$Min\ \underline{Z} = \sum_{t}\{\textbf{\textit{First - stage}}\} + \alpha \tag{30}$$

$$\alpha \geq \underline{\alpha} \tag{31}$$

$$\sum_{g} P^{0}_{g,t} + \sum_{w}(P^{0}_{w,t} - WS^{0}_{w,t}) + \sum_{e} P^{0}_{e,t} = D^{0}_{n,t} \tag{32}$$

(2)-(5), (10)-(19), (23)-(24), (26)-(29), (33)

Constraint (31) imposes a lower bound on to accelerate convergence. The power balance equation for the base case is given in (32). Constraint (33) enforce all base case (s=0) constraints. Other unit constraints including minimum on/off time, ramping up/down rate limitations are considered here [13].

First Sub-problem (Hourly Network Evaluation for the Base Case): The hourly network evaluation checks possible network violations of the master solution, specific possibility of a feasible TS solution for the base case.

The objective is (34):

$$Min\ W^{0} = \sum_{t}\overbrace{\left(\sum_{n}(MP^{0}_{1,n,t} + MP^{0}_{2,n,t})\right)}^{W^{0}_{t}} \tag{34}$$

The bus power mismatch is presented by (35), where $MP^{s}_{1,n,t}$ and $MP^{s}_{2,n,t}$ are surplus and deficit variables. The mismatch of power balance should be minimized as shown in (34). Constraint (36) comprises the base case constraints. Decision variables in constraints (37)–(44), are the fixed values calculated by the master problem. Also, in (37)-(44), the arrow denotes the dual variables of the equality constraints for feasibility cuts. Note that, in base case for constraints (37)-(44) is for $s = 0$.

$$\begin{aligned}\sum_{\forall g(n)} P^{0}_{g,t} + \sum_{\forall w(n)} P^{0}_{w,t} + \sum_{\forall e(n)} P^{0}_{e,t} \\ + \sum_{\forall k(.,n)} P^{0}_{k,t} - \sum_{\forall k(n,.)} P^{0}_{k,t} = D^{0}_{n,t} + MP^{0}_{1,n,t} - MP^{0}_{2,n,t}\end{aligned} \tag{35}$$

(11)-(12), (26)-(29) (36)

$$P^{0}_{g,t} = \hat{P}^{0^{(v)}}_{g,t} \rightarrow \gamma^{s^{(v)}}_{g,t}, \quad \gamma^{(v)}_{g,t} = \sum_{s}\pi_{s}\gamma^{s^{(v)}}_{g,t} \tag{37}$$

$$u_{g,t} = \hat{u}^{(v)}_{g,t} \rightarrow \eta^{s^{(v)}}_{g,t}, \quad \eta^{(v)}_{g,t} = \sum_{s}\pi_{s}\eta^{s^{(v)}}_{g,t} \tag{38}$$

$$D^{0}_{n,t} = \hat{D}^{0^{(v)}}_{n,t} \rightarrow \lambda^{s^{(v)}}_{n,t}, \quad \lambda^{(v)}_{n,t} = \sum_{s}\pi_{s}\lambda^{s^{(v)}}_{n,t} \tag{39}$$

$$SR_{n,t}^{up} = S\hat{R}_{n,t}^{up(v)} \rightarrow \vartheta_{n,t}^{s(v)}, \quad \vartheta_{n,t}^{(v)} = \sum_s \pi_s \vartheta_{n,t}^{s(v)} \tag{40}$$

$$SR_{n,t}^{dn} = S\hat{R}_{n,t}^{dn(v)} \rightarrow \xi_{n,t}^{s(v)}, \quad \xi_{n,t}^{(v)} = \sum_s \pi_s \xi_{n,t}^{s(v)} \tag{41}$$

$$SR_{g,t}^{dn} = S\hat{R}_{g,t}^{dn(v)} \rightarrow \zeta_{g,t}^{s(v)}, \quad \zeta_{g,t}^{(v)} = \sum_s \pi_s \zeta_{g,t}^{s(v)} \tag{42}$$

$$SR_{g,t}^{dn} = S\hat{R}_{g,t}^{dn(v)} \rightarrow \psi_{g,t}^{s(v)}, \quad \psi_{g,t}^{(v)} = \sum_s \pi_s \psi_{g,t}^{s(v)} \tag{43}$$

$$z_{k,t} = \hat{z}_{k,t}^{(v)} \rightarrow \mu_{k,t}^{s(v)}, \quad \mu_{k,t}^{(v)} = \sum_s \pi_s \mu_{k,t}^{s(v)} \tag{44}$$

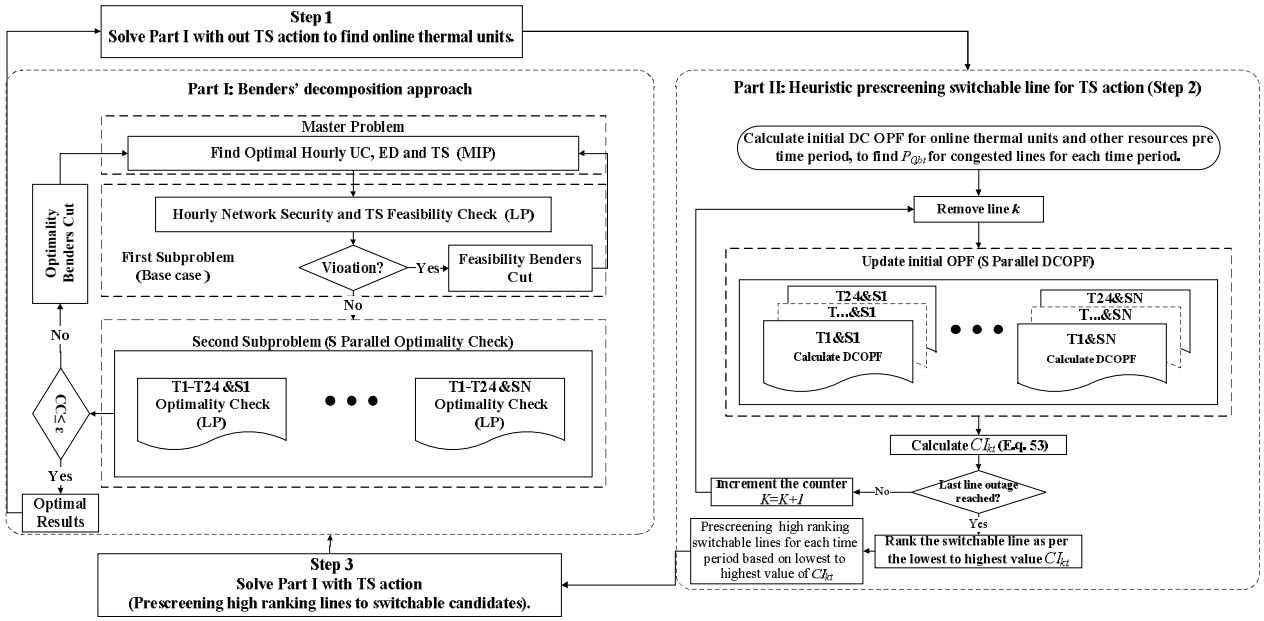

Fig. 1. Proposed accelerating decomposition technique; CC: convergence check.

The feasibility Benders cut (45) will be created and imposed by the master problem for the solution of the next iteration, when violations occurred in scenarios, i.e., W_t^0 is higher than a specified threshold:

$$\begin{aligned}
&\hat{W}_t^{0(v)} + \sum_g \gamma_{g,t}^{0(v)} (P_{g,t}^0 - \hat{P}_{g,t}^{0(v)}) + \sum_g \eta_{g,t}^{0(v)} (u_{g,t} - \hat{u}_{g,t}^{(v)}) \\
&+ \sum_n \lambda_{n,t}^{0(v)} (D_{n,t}^0 - \hat{D}_{n,t}^{0(v)}) + \sum_k \mu_{k,t}^{0(v)} (z_{k,t} - \hat{z}_{k,t}^{(v)}) \\
&+ \sum_n \vartheta_{n,t}^{0(v)} (SR_{n,t}^{up} - S\hat{R}_{n,t}^{up(v)}) + \sum_k \xi_{n,t}^{0(v)} (SR_{n,t}^{dn} - S\hat{R}_{n,t}^{dn(v)}) \\
&+ \sum_n \xi_{g,t}^{0(v)} (SR_{g,t}^{up} - S\hat{R}_{g,t}^{up(v)}) + \sum_k \psi_{g,t}^{0(v)} (SR_{g,t}^{dn} - S\hat{R}_{g,t}^{dn(v)}) \le 0
\end{aligned} \tag{45}$$

Second Sub-problem (Optimality Check for Each Scenario): The sub-problem for scenario s and time period *t* is formulated as (46)-(48):

$$Min\ Z^s = \sum_t \overbrace{\left[\begin{array}{l}\sum_g(\sum_i \lambda^G_{i,g,t}\cdot\Delta r^s_{i,g,t}) + \sum_n\sum_j(\lambda^D_{j,n,t}\cdot\Delta d^s_{j,n,t}) \\ +\sum_n \rho_n \cdot LS^s_{n,t} + \sum_w \rho_w \cdot WS^s_{w,t}\end{array}\right]}^{Z^s_t} \quad (46)$$

$$(6)\text{-}(12),\ (20)\text{-}(29) \quad (47)$$

$$(37)\text{-}(44)\ for\ s>0 \quad (48)$$

The optimality check sub-problem (46)-(48) checks the optimality of master solution in scenario *s* and time period *t*. The objective function (46) represents total operation costs in real time operation. Constraint (47) contains the second-stage constraints. Constraints (48) fix the values of the complicating variables to given values achieved from the solution of the master problem. The complicating variables are fixed through constraints (37)-(44), whose dual variables, provide sensitivities to be used in building optimality Benders' cuts for the master problem. Note that, here for constraints (37)-(44) is for $s>0$.

Convergence check: The upper bound for the optimal value of objective function of the original problem (1)–(29) at iteration v is obtained as follows:

$$Z^v = \sum_t\sum_s \pi_s Z_t^{s^{(v)}} \quad (49)$$

$$\overline{Z}^v = Z^v + \sum_t \{\textbf{\textit{First - stage}}\} \quad (50)$$

where the value of $\{\textbf{\textit{First - stage}}\}$ is calculated by using the fixed variable in constraints (37)-(44).

$$\left|\overline{Z}^v - \underline{Z}^v\right| \le \varepsilon \quad (51)$$

If the value of (51) is not lower than the level of accuracy ε, the optimality cut (52) will be utilized for the master problem:

$$\begin{array}{l} Z^{(v)} + \sum_g \gamma^{(v)}_{g,t}(P^0_{g,t} - \hat{P}^{0^{(v)}}_{g,t}) + \sum_g \eta^{(v)}_{g,t}(u_{g,t} - \hat{u}^{(v)}_{g,t}) \\ +\sum_n \lambda^{(v)}_{n,t}(D^0_{n,t} - \hat{D}^{0^{(v)}}_{n,t}) + \sum_k \mu^{(v)}_{k,t}(z_{k,t} - \hat{z}^{(v)}_{k,t}) \\ +\sum_n \vartheta^{(v)}_{n,t}(SR^{up}_{n,t} - \hat{SR}^{up^{(v)}}_{n,t}) + \sum_k \xi^{(v)}_{n,t}(SR^{dn}_{n,t} - \hat{SR}^{dn^{(v)}}_{n,t}) \\ +\sum_n \xi^{(v)}_{g,t}(SR^{up}_{g,t} - \hat{SR}^{up^{(v)}}_{g,t}) + \sum_k \psi^{(v)}_{g,t}(SR^{dn}_{g,t} - \hat{SR}^{dn^{(v)}}_{g,t}) \le \alpha \end{array} \quad (52)$$

A. The second part (Heuristic prescreening of switchable lines)

Network congestion in a power system limits the resource output of cheaper producing resource and increases the output of more costly resources. The TS action has the potential to bring in additional available transfer capability to transmit more power from lower-cost producing resources to meet the system load. The TS action can therefore reduce the total operating cost of a system. In mathematics, the TS action is a mixed integer programming (MIP) problem [38].

Solving the MIP problem is not as easy as solving a SSCUC problem with TS action because binary variables as well as big-M constraints introduce more computational complexity. The branch-and-cut algorithm is the most commonly used and most effective method to solve the MIP problem. However, the generated branch-and-bound tree and cutting planes needed to solve the problem is usually too large to store. So, even commercial solvers, like CPLEX, fail because they run out of memory. This part, describe a prescreening method used to select a limited number of line candidates from the set of all the transmission branches to reduce the number of integer variables in the MIP problem. Also, due to excessive execution times for large-scale systems, the switchable lines are specified by some heuristics method, such as a pre-screening method. The pre-screening method can be used to select a few switchable line candidates, reducing the number of binary variables in proposed SSCUC problem with TS action. In addition, it could reduce the computational burden, significantly.

Heuristic prescreening of switchable lines for the TS action:

Solving the TS action when there are a huge number of candidate lines is extremely complex. In this paper, to overcome this issue, a strategy to do prescreening of a few switchable line candidates for TS action is used. The idea behind this strategy is that switching off a line can reduce power flow on congested lines. The new system topology has the potential to bring in additional available transfer capability to increase power injections from cheaper resources and reduce power injections from the more expensive resources. An index CI_{kt} , in (53), is considered to appraise the relative difference between the power flow of congested transmission lines before and after TS action.

The congested transmission lines are described by setting K^* in (53) includes all congested lines (e.g., lines loaded at 100% of their limit capacity) and nearly congested lines (e.g., lines loaded above 90% of their limit capacity) because some lines loaded close to their capacity's limits before switching may become overloaded after a line *k* is switched action. Let $P_{0,bt}$ denote the power flow through congested line *b* at time period *t*, determined by solving SSCUC problem with the original transmission lines topology in (step 1). Where, ΔP_{bt}^{s} denotes the power flow change on congested lines caused by switching line *k* at scenario *s* and time *t*. Entirely switchable line candidates in the set $\left\{CI_{kt}, \forall k \in K^*\right\}$ are ranked from the lowest number to the highest number for each time period *t*. Equation (53) given ranking of switchable line candidates:

$$CI_{kt} = \sum_{s} \sum_{b \in K^*} \frac{\overbrace{P_{bt}^{s} - P_{0,bt}^{s}}^{\Delta P_{bt}^{s}}}{P_{0,bt}^{s}}, \quad k \in K^* \tag{53}$$

The proposed accelerating solution strategy is given as follows:

Step 1) The SSCUC problem (i.e., (30)-(52)) without transmission switching (i.e., all binary variables are fixed to one) solved by the BD method, then obtained the 24-h thermal unit commitment, $u_{g,t}$, and $P_{0,bt}$ the power flow through congested line *b* at time period *t* and scenario *s*.

Step 2) The part II of Fig. 1 is started. In this step, the binary variables for demand *n*, thermal unit *g,* and the ES system *e* variables (i.e., u_{nt}, u_{gt} and u_{et}) are fixed to their solution values from the first part (Part I). Then, DC OPF model (1)-(29) without TS action is solved repeatedly again, each time with one of the lines removed from service; for each single line removed, the DCOPF is run to obtain P_{bt}^{s} for all the congested lines and calculate CI_{kt} by (53). Finally, the lines are ranked based on the calculated CI_{kt}.

Step 3) Finally, the first part (Part I) should be run to solve the SSCUC problem with TS action based on the selected lines by prescreening switchable lines in part II and other flexibility resources, then the process of solution problem has been stopped.

V.Numerical Studies

The proposed stochastic SCUC is applied to the 6-bus test system and the IEEE 118-bus large-scale system to evaluate the performance of the proposed solution strategy. The simulations have been implemented using CPLEX 12.3.0 under GAMS [39] on a personal computer with Core i7 CPU running at 3.4-GHz and 32 GB of RAM.

A. Six-Bus System

The 6-bus system illustrated in Fig. 2 has three thermal units, seven transmission lines, and three demands. The thermal units from most expensive to cheapest are G3, G1, and G2. The thermal units from high to low flexibility are G3 (quick-start unit) and G1 (higher the value of $P^{\min}$). The SR prices are 10, 14, and 8 $/MWh for three units, respectively. The lines flow limit for the lines 2-4 and 4-5 is 40 MVA and is 150 for all other lines. The storage unit has been connected to bus 5. The hourly demand, storage parameters, ramp rates and quadratic cost coefficients are taken from [13]. The WPG unit with a maximum power output of 110 MW is installed at bus 2, which is about 43% of the system peak load. The percentage of available WPG for each hour is given in Fig.3.

The cost of WPS is 100 $/MWh that is higher than the largest marginal cost of the existing thermal units. The responsive demand bid consists of a single energy block with a bidding price of 20 $/MWh. The minimum hourly and maximum daily load shedding are considered to be of 1 MWh and 100 MWh for all demands, respectively. The minimum up/down times are 4 hours and the demand up/down rates are considered to be large enough to allow any demand changes in successive hours. Accordingly, based on this assumption, the DS has high flexibility. Load participation factor (LPF), is an indicator of the customer demand flexibility (e.g., higher LPF relates to more responsive loads and higher DS flexibility [17]).

All of the demands offer to sell ‘up/down SR at 20 $/MWh and the deployment cost of SR for each demand is 15 $/MWh. In this paper, due to limited up/down ramp rate of thermal units, they provide low flexible reserve resource and due to high up/down rates of demand, they can provide higher flexible reserve resources. The value of lost load (VOLL) is 500 $/MWh for all of the loads. Using the MCS, 2000 scenarios are generated and scenario reduction techniques are used to obtain 15 scenarios. The following five cases are studied to manage uncertainty with flexibility from the SS and other flexibility resources as follows: Case 0: The DS flexibility is applicable at all demands (with LPF=0.2).

Case 1: Case 0 (with LPF=0.9).

Case 2: Case 0 and the NS flexibility.

Case 3: Case 0 and the SA flexibility.

Case 4: The DS, SA and NS flexibility.

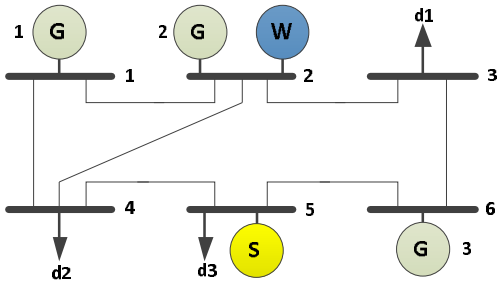

Fig. 2. One-line diagram for the six-bus system.

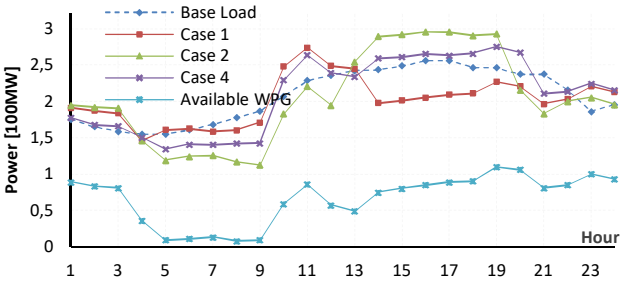

Fig. 3. Comparison of WPG output and daily load profile.

These cases are discussed as follows.

Case 0: This case provides a reference in which the DR program is considered. The EOC is $123812.56. Table II depicts the scheduling of three thermal units. G1 is scheduled to generate between hours 7–22, while G2 and G3 are scheduled at all hours since they are the cheapest and the highest flexible units, respectively. The total SSR, DSR,

expected wind power spillage (EWPS), i.e., $\sum_t \sum_s \sum_w \rho_s \cdot WS_{w,t}^s$, and expected energy not supplied (EENS), i.e., $\sum_t \sum_s \sum_n \rho_s \cdot LS_{n,t}^s$ are given in Table II.

Case 1: As shown in Table II, in case 1, the flexibility from the DS is increased from LPF=0.2 to LPF=0.9. For this reason, the EOC is decreased from \$123812.56 (case 0) to \$109127.25 (case 1). Also, the commitment of G1, less flexible unit, and G3, expensive unit, are decreased from 16 and 24 hours in Case 0 to 10 and 19 hours in Case 1, respectively. In addition, by comparing Cases 0 and 1 in Table III, the SSR (as a less flexible resource) is decreased from 510.56 MWh to 433.17 MWh and DSR (as a highly flexible resource) is increased from 915.21 MWh to 1052.70 MWh. All in all, the total reserve resource (SSR plus DSR) in the system is increased from 1425.77 MWh to 1485.87 MWh in cases 0 and 1, respectively. In the case 1, with a higher flexibility from DS (LPF=0.9), the system demand profile would almost follow the behavior of the hourly WPG profile (as shown in Fig. 3). As shown in Fig. 3 the DR in case 1 causes load profile is approximately paralleled in most hours with the WPG profile. Therefore, comparing cases 0 and 1, the EWPS is decreased by 58.44%, i.e., from 101.31 MWh in case 0 to 42.10 MWh in case 1. These results show that in case 1 the WPG variability is more compensated by the DR and DSR. In addition, as shown in Table III, the EENS in case 1 will be reduced in comparison with case 0 by 35% when total reserve capacity is increased in the network.

Case 2: The cheaper G2 is on at all hours while G1 is used at peak hours to satisfy the remaining load and minimize the EOC. Furthermore, since the wind farm is installed in bus 2, with more WPG, the power through the lines connected to bus 2 are increased. In this condition, power flowing through lines 2-4, 2-3 and 4-5 will be violations. Therefore, expensive G3 is committed to helping alleviate these violations. Lines 2–4 and 2-3 are congested at hours 7–22, which leads to a lower dispatch of G2 and wind farm and a higher EOC. In order to lower the power flowing on these lines, two primary option are usually utilized: WPS or/and load shedding. Load shedding at buses 3, 4 and 5 would lead to a decrease in the flow of Lines 2-4, 2-3 and 4-5. Also, WPS at bus 2 would result in a decrease in the flow of the congested lines 2-4 and 2-3. Since load shedding is supposed to be an expensive option here, WPS would be the profitable choice. Using TS can reduce the hourly commitment of expensive G3 and low flexible G1 units. The G2 is scheduled at all hours since it is the cheapest unit. The commitment of G1 and G3 are decreased from 16 and 24 hours in Case 0 to 12 and 15 hours in Case 2, respectively. For this reason, the EOC is decreased from \$123812.56 in case 0 to \$117295.43 in case 2. For example, at hours 8-14 when lines 2-4, 2-3 and 4-5 are congested, lines 2–4 and 4–5 are switched off instead of committing unit 3. Here, there will be no transmission loop residual in the six bus system and the remaining lines could increase the flows to their limits, (in Fig.2.). Table IV shows the state of switchable lines in which lines 2–4 and 4–5 are mostly switched off. At peak hours 17-20, the security constraints cannot be satisfied without placing back the lines 2–4 and 4–5. Also, the TS action as an effective and powerful tool can facilitate the DR

program with even in the case of the less flexible demand side (i.e., LPF=0.2). Comparing the case 0 with the case 2, it can be inferred that the TS caused the reduction of SSR from 510.56 MWh to 378.53 MWh and the increment of DSR from 915.21 MWh to 1281.34 MWh, respectively. In Table III, by considering both DR and TS (Case 2), the system would have the higher wind power absorption capacity, that is, EWPS in case 2 would decrease 74.6% and 39% with respect to the cases 0 and 1, respectively. As shown in Fig. 3 the DR and TS in case 2 causes load profile is approximately paralleled in some hours (i.e., hours 1-13 and 20-24) with the WPG profile. Also, comparing case 1 and case 2, it would be found that TS and DR (case 2) have more influence on the EWPS reduction than higher flexible DS system (case 1). Moreover, in Table III, the EENS is decreased 35% in case 1 and 18% in case 2 in comparison with case 0, which indicates the higher LPF (case 1) is more effective to reduce EENS than the network reconfiguration.

Case 3: The ES unit, in this case, would improve the implementation of DR. ES system and DR can optimize commitment of dispatchable units. For instance, the commitment of G1, as a lower flexible unit, is decreased from 16 hours in case 0 to 11 hours in case 3. Thus, the ES unit enhances the flexibility of the system. According to Table II, the EOC has been decreased by 3.8% in case 3 compared with case 0. Also, as shown in Table III, the ES unit and DR reduced the EWPS but in comparison with case1 and 2 the EWPS is less reduced due to the existence of congestion. However, the ES unit in case 3 can be the best option to reduce the EENS. For example, in Table III, in comparison with case 0, the EENS is more reduced in case 3 than cases 1-2. In this case, the SSR and DSR are increased by 6% and 16.8% in comparison with case 0. Thus, compared with case 0, cases 1 and 2 would bring more flexibility than case 3.

Case 4: In this case, the shortcomings of case 3 are resolved by employing TS action. The TS action by changing network configuration can relieve congestion and increase the efficiency of ES unit. The changes in the hourly switchable line states in case 4 compared to case 2, are highlighted in Table IV. Note, highlighted numbers mean the state should be changed with respect to case 2. However, in this case, both switchable lines 2–4 and 4–5 will be switched off for the entire daily time due to the existence of storage facilities as compared to case 2. In case 2 and case 4, all lines are considered as switchable. Nevertheless, only lines 2–4 and 4–5 are switched in these cases. In Fig.3., switching off any of lines 2–3, 3–6, 4–5, and 5–6 will remove the loop 2–3–4–5–6–2 with better results. Since line 4–5 has the lowest capacity, it is often subject to congestion which makes the line a good candidate for switching. This conclusion is consistent with the proposed results. By switching off the line 4–5, the line flow in the loop, i.e., those of lines 2–3, 3–6, and 5–6, can be increased without affecting the flow of other transmission lines. Next line, switching off any of lines 1–2, 1–4 and 2–4, from loop 1–2–4–1, could be a good choice for next switching line. Since G1 is the largest unit, it will remain in service along with the attached lines. So, line 2–4 would be the best TS select for this loop. With switching off both lines 2–4 and 4–5, there are still enough lines coupled to bus 4 to supply its load. By considering lines 2–4 and 4–5 as switchable, loops would be relaxed while meeting the load balance requirements. In Table II, the commitment of G3 is decreased from 24 hours in case 3, to 15 hours in case 4, due to increase in system

flexibility. As shown in Fig. 3 in case 4, the DR, the TS action and the ES unit causes load profile is approximately paralleled in entire hours with the WPG profile. For this reason, comparing cases 0 and 4 in Table III, the EWPS is decreased by 95.7% from 101.31 to 4.33 MWh, respectively. It means in comparison with cases 1-3 the EWPS is more reduced in case 4. Here, the WPG variability is compensated by the ES unit and thermal generating units. In entire flexible option proposed in this paper, the TS action (in cases 2 and 4) is the best option to reduce WPS. Also, in comparison with case 0, the EENS is reduced by 85.4% in case 4, which is the highest reduction in all cases. Finally, based on Table III, the EOC in case 4 is more reduced than cases 0-3.

Table II

Hourly Commitment in Case 0-4

Case 0	**Units Always Online: G2,G3, EOC ($) : 123812.56**
Unit	**Hours (1-24)**
G1	0 0 0 0 0 0 1 1 1 1 1 1 1 1 1 1 1 1 1 1 0 0
Case 1	**Unit Always Online: G2, EOC ($) : 109127.25**
Unit	**Hours (1-24)**
G1	0 0 0 0 0 0 0 0 0 0 0 0 1 1 1 1 1 1 1 1 0 0
G3	1 1 1 1 0 0 0 0 0 1 1 1 1 1 1 1 1 1 1 1 1 1
Case 2	**Unit Always Online: G2, EOC ($) : 117295.43**
Unit	**Hours (1-24)**
G1	0 0 0 0 0 0 1 1 1 1 1 1 1 1 1 1 1 0 0 0 0 0
G3	0 0 0 1 1 1 1 0 0 0 0 0 0 1 1 1 1 1 1 1 1 1
Case 3	**Units Always Online: G2,G3 EOC ($) : 119089.76**
Unit	**Hours (1-24)**
G1	0 0 0 0 1 1 1 1 1 1 1 1 1 0 0 1 1 0 0 0 0 0 0
Case 4	**Unit Always Online: G2, EOC ($) : 98782.89**
Unit	**Hours (1-24)**
G1	0 0 0 0 0 0 1 1 1 1 1 0 0 0 1 1 1 1 0 0 0 0 0
G3	1 1 1 1 1 1 1 1 1 1 1 1 1 1 1 0 0 0 0 0 0 0 0

Table III

Comparison of Result for Case 0-4

WFE (%) = 20	**Case 0**	**Case 1**	**Case 2**	**Case 3**	**Case 4**
SSR (MWh)	510.56	433.17	378.53	543.56	413.72
DSR (MWh)	915.21	1052.70	1281.34	1100.00	1531.22
EENS (MWh)	40.50	26.31	33.56	15.34	5.89
EWPS (MWh)	101.31	42.10	25.68	56.46	4.33

Table IV

Switchable Line Schedule of Six-bus System in Cases 2 and 4

Line	Hours (1-24)
2-4	1 1 1 1 1 0 0 0 0 0 0 0 0 0 0 1 1 1 1 1 0 0 0 0
4-5	1 1 1 1 1 0 0 0 0 0 0 0 0 0 0 1 1 1 1 1 0 0 0 0

B. Modified IEEE 118-Bus System

The modified IEEE 118-bus system is a large-scale power system with 54 thermal generators, 186 branches, and 91 load buses. Parameters of generators, transmission network, and load profiles are given at [motor.ece.iit.edu/data/SCUC_118]. However, the line flow limits for a few lines are reduced to 100 MW to enforce the system congestion in the simulations. There are 3 geographically dispersed WPG at buses 15, 54, and 96. The WPG capacity is 1200 MW. The percentage of hourly load system is the same as the previous six-bus system where the peak demand is 3733.07 MW at hour 17. The installed WPG is 32.1% of the system peak demand. The wind output profile of the WPG units follows the same pattern as that of the six-bus system. Three ES units are installed at buses 17, 49 and 80 follow the same capacity and parameters of the previous six-bus system. The VOLL is set at 500 $/MWh. Using the MCS, 1800 and 10000 scenarios are generated and scenario reduction techniques are used to obtain 10 and 100 scenarios [37]. The three cases, which were studied in the previous system, are examined for this system as well. Table V and Fig.4, shows the EOC, SSR, DSR, and EENS in different cases. The results in Table V are consistent with those of the previous system. The EOC, the SSR, less flexible reserve resource, and EENS have the lowest values in case 4. In addition, the DSR (high flexible reserve resource) has the highest value in case 4, that is, TS and ES units would be efficient tools to compensate the uncertainty of WPG and component failure in the large system.

Fig. 4 shows EWPS in cases 0, 2, 3 and 4. In this figure, the WFE is varied starting from 5% to 30%. Here, the sensitivity of the EWPS to WFE is significant in WFE>15%, because, the required reserve (e.g. SSR or DSR) would be high as the WFE is increased at the high penetration level of WPG and it is not economic. However, by adding flexible options (e.g., ES unit or TS action) to the system, the EWPS is reduced. For example, compared with case 0, the EWPS in case 2 is decreased by incorporating TS with DR program. Also, the EWPS in case 4 is more decreased as compared to cases 0, 2 and 3. It can be inferred that when the DR, TS and ES (case 4) are considered, the system would have the highest wind power absorption capacity. Not that in the proposed bender's decomposition (BD) technique, the solution time needed to solve each second sub-problem is about to 1.5% of the total solution time, which is reasonable. For this reason, as shown in Table V, in case 0, case 2, case 3 and case 4, with increasing number of scenarios from 10 to 100

the computational time not significantly increase for a comparatively large-scale system. This means that proposed BD technique is suitable for a larger number of scenarios in a comparatively large-scale system.

C. Modified IEEE 300-Bus Large-Scale System

The IEEE 300-bus test system as a more realistic and larger test system is used here, just to represent the computational times required for our proposed solution strategy (PSS) against the scale of the test system. It consists of 69 generators, 411 transmission lines with the total load of 23525.8 MW. The percent of the hourly load is the same as previous test systems. The IEEE 300-bus test system as a more realistic and larger test system is used here, just to represent the computational times required for solving stochastic SCUC problem against the scale of the test system.

Data for this system are available in [Available: http://khorshid.ut.ac.ir/h.ahmmadi/download.htm]. The wind power units are added to Buses 81 (wind farm 1), 130 (wind farm 2) and 198 (wind farm 3). The wind farm profile of the unit located at bus 81 follows the same pattern as that of the wind farm 1, 2 and 3 in the previous system which is scaled by the factor of twenty. Three ES systems are set up at buses with wind farms that following the same capacity and parameters of the previous six-bus system, but, is scaled by the factor of two.

Table V

Comparison of Results for Different Cases in the 118-Bus System

NS	WFE=15%	Case 0	Case 2	Case 3	Case 4	CT [min]
10	**EOC(1000$)**	1191.1	1087.8	1098.1	899.4	C0=5 C2=15 C3=8 C4=25
	SSR (MWh)	5867.5	3864.2	3971.3	3431.6	
	DSR (MWh)	6783.4	9037.3	8989.9	14532.1	
	EENS (MWh)	279.5	267.1	241. 79	32. 8	
100	**EOC(1000$)**	1226.7	1102.5	1173.1	914.3	C0=25 C2=60 C3=32 C4=90
	SSR (MWh)	5925.1	3918.9	4145.6	3503.4	
	DSR (MWh)	6822.7	9101.4	8976.3	15231.4	
	EENS (MWh)	299.1	294.6	257. 1	43. 2	

NS: Number of scenarios, **CT**: computation time ,**C0**:case0, **C2**:case2, **C3**: case 3 **C4**:case4

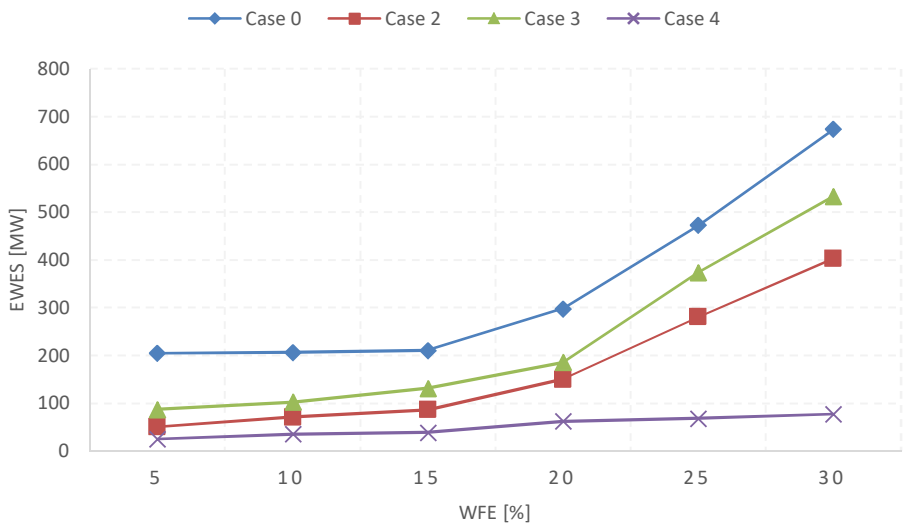

Fig. 4. The EWPS as a function of WFE.

The WPG forecast errors and equipment failure (unit/line) are represented by 2000 Monte Carlo scenarios. The number of scenarios is reduced to 20 by using forward-backwards scenario reduction techniques. The Case 4, which were studied in the previous system, are examined for this system as well. The results obtained from the PSS for solving the SSCUC problem on the IEEE 300-bus test system are presented in Table VI and compared with the results obtained from three other solution approaches that proposed in references [3], [6], [10], and [19]. As shown in Table VI, the solution strategy proposed in reference [19] can solve our SSCUC problem with all of the flexibility resources (especially with TS action), for this test system with too many Benders iterations. Because the TS action plays an important role in the long computing time, even for the DC-based model. In this reference, the general BD method is proposed for solving the SSCUC problems. The main disadvantage of the general BD method to solve our proposed problem, with a large number of the TS action, too many iterations needed to achieve convergence. Then, its solution takes too much CPU time. On the other hand, due to the master problem of the BD technique in this reference include both first- and second-stage variables. This fact is very important because the master problem grows significantly, with each iteration, especially in this test system with a large number of switchable lines. Table VI also shows that the solution strategy proposed in reference [19] has considerably high computation time and leads to the worst expected cost among all of the methods of this Table. Among the next three methods of Table VI that can solve the SSCUC problem for IEEE 300-bus test systems, the PSS obtains the lowest expected cost and computation time with the lowest GAP compared to other solution strategies, and considerable differences are seen between the PSS and other solution strategies of Table VI.

The results obtained from the proposed solution strategy (PSS) for solving the SSCUC problem on the IEEE 118/300-bus test system are presented in Table VII and compared with the results obtained from on other MIP solution

approaches. The first solution methods of Table VII, that is, CPLEX, is a well-known MIP solvers of GAMS software package [39]. Thus, the CPLEX cannot solve the SSCUC problem for these test systems as shown in Table VII. Table VII shows that results obtained from PSS method have the lowest expected cost with lowest computation time and reasonable GAP, i.e., 0.2%.

Note that the overall solution time of the decomposed method increases with the system size. This can be observed from the results presented in Tables VII. For instance, comparing the computation time results of the 118-bus, and 300-bus systems for SSCUC model, in post TS action, it becomes evident that the solution time of the 300-bus system is nearly 3.5 times larger than the 118-bus system. While system size increases with a factor of 2.5 the corresponding solution time for SSCUC model increase in a linear manner with the system size.

To show the effectiveness of the PSS for the proposed SSCUC model in handling a larger number of switchable lines, the effect of using the accelerating PSS with and without part II is studied. The number of switchable lines is increased from 5 to 40. The optimality gap of CPLEX is 0.02% for the stopping criterion. The EOC value and computation time for the PSS with and without part II for different numbers of switchable lines are achieved and displayed in Fig. 5. In addition, the EOC value and computation time obtained from solution strategy proposed in reference [6] are displayed in this figure. As shown in Fig.5, the PSS without part II cannot handle our proposed program with a large number of switchable lines, i.e., more than 10 candidate switchable lines. Also, as can be seen in Fig 5, the EOC value would not be reduced for more than 10 candidate switchable lines for the PSS without part II and the solution strategy proposed in reference [6]. Also, the PSS would accelerate the large-scale problems to find optimal solutions in a reasonable computation time. Also, as shown in Fig. 5, the computation time for the decomposed model with part II is reduced more than the PSS without part II. For example, for 40 switchable lines, the PSS with/without part II for SSCUC problem finds the optimal solution in <139 min and >410 min, respectively.

It should be noted that above solution times are obtained using serial computation on a simple hardware set (8 Quad-Core processors clocking at 3.4 GHz with 32 MB RAM). In other words, all scenarios are sequentially solved on this personal computer. From the above table, it is seen that, despite of relatively real network size of the IEEE 118/300 bus test system, the dimensions of the proposed scheme are high which leads to the high computation time. Though, some simplifications can be made to mitigate this dimensionality issue. These simplifications can be summarized as follows [40] and [41].

- A zonal approach could be used instead of representing the full grid, wherein only the transmission links between a restricted number of areas are modeled.

- Reducing the number of contingencies using advanced scenario reduction techniques can also lower the dimensionality, under the philosophy that it is better to consider a few significant contingencies than none at all.

to consider a few significant contingencies than none at all.

Also, the proposed approach is well-suited for parallel processing computer systems. Furthermore, it is noted that the above results for the stochastic SCUC are outcomes of prototype software executed on a simple hardware set in our lab, since we would like to present the underlying ideas. To convert a prototype computer code to an industrial software package, usually the written code is optimized by different software techniques to modify its memory use, reduce computation burden, etc. Moreover, ISOs usually have much better computers for stochastic SCUC process than our simple hardware set. At the end, please note to this explanation quoted from [41]: "Not to be neglected are the constant improvements in the cost and performance of computing machinery and optimization codes. These allowed the development of the current ISOs in the United States—something not conceivable 20 years ago."

The following computational, optimality and implementation issues are in order:

- The computational times required for solving the IEEE 300-bus and IEEE 118-bus test system with 20 scenario are given in Table VII. The proposed technique is feasible for realistic size networks. Note that CPU time varies fairly linearly with the number of buses. Computational times are reasonable considering that a design problem is solved. Also, the CPU time increases significantly with a smaller value for, GAP=0.1%.
- Note that reducing the number of scenarios is computationally appropriate if decomposition techniques are not used, while a larger number of scenarios is generally better if decomposition techniques are used. It is important to note that using a larger number of scenarios generally results in higher accuracy.
- The pre-screening methods described can be used to select a few switchable line candidates, reducing the number of integer variables in transmission switching problems. The simulation results indicate that the proposed prescreening methods can reduce the time needed for solve stochastic SCUC to find better feasible solutions.

However, to tackle case studies pertaining to real-world systems with thousands of nodes and lines and a large number of scenarios, the following additional alternatives are also available:

- To use a supercomputer,
- To implement parallelization techniques [42],
- To apply appropriate techniques to simplify the network and/or to reduce the number of scenarios [43],
- To decompose the AC-SCUC problem by area [27].

Table VI

Comparing results of other decomposed method proposed in other references with our PSS, with 10 switchable lines

Refs	EOC (M$)	CPU time (min)/ Gap (%)	Benders iterations
[10]	85278920	320/0.2	65
[6]	85075214	300/0.2	43
[3]	81956415	220/0.2	21
[19]	91856691	650/0.2	98
PSS with Part II	81178920	130/0.2	11

Table VII: Obtained results for stochastic SCUC problem on IEEE 118 and 300-bus test system by proposed solution strategy, with 10 switchable lines, for Case 4.

Test systems	**Solution approaches**	Expected costs [$]	GAP [%]	Time [min]
IEEE 118-bus	CPLEX	No answer	-	-
IEEE 300-bus	CPLEX	No answer	-	-
IEEE 118-bus	PSS with Part II	906492	0.1	37
IEEE 300-bus	PSS with Part II	81178920	0.1	130

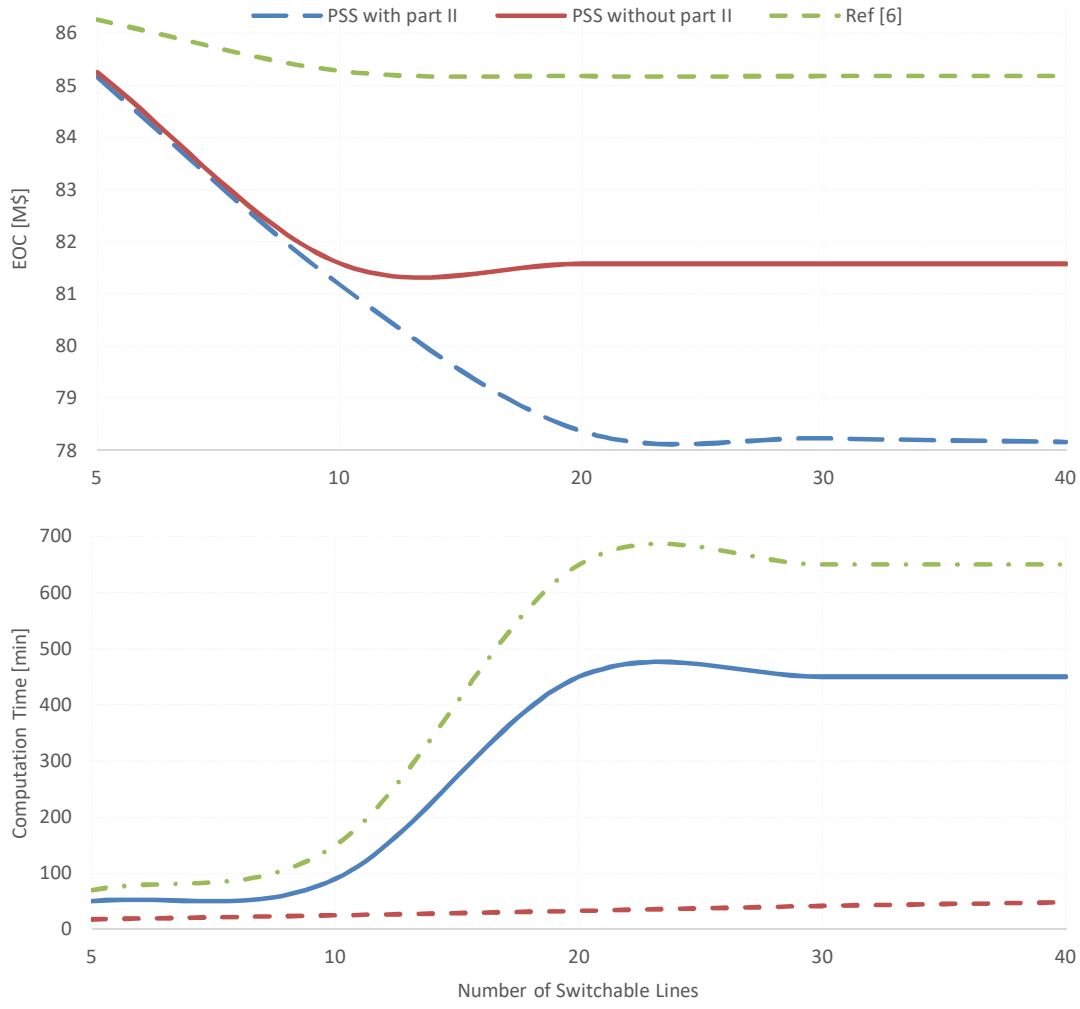

Fig. 5. Computation time and EOC comparison of PSS without and with part II, and reference [6].

VI. Conclusion

Coping with high penetration wind power uncertainty calls on higher flexibilities of various resources. A stochastic SCUC scheduling model with multiple flexibility resource options was proposed in this paper, which included DR, TS, and ES units in an innovative integrated scheme. Numerical results demonstrated that with increased system flexibility, the EWPS and EOC decreased. Also, in this paper it was shown that the highest flexible system with the lowest EWPS and EOC would be obtained by combining DR, TS and ES units in the power system. Furthermore, results indicated that TS could play an important role in facilitating DR programs even with less LPF. For example, given the same demand and available WPG, the TS in some cases with less LPF accommodated more WPG (i.e. less wind curtailment) compared with some cases with high LPF. Hence, this paper provided an accelerating and efficient solution method to solve the SSCUC problem with flexibility resources and under uncertainty. The numerical results obtained clearly demonstrated and validated the proficiency of the proposed accelerating solution strategy.

VII. Acknowledgment

J.P.S. Catalão acknowledges the support by FEDER funds through COMPETE 2020 and by Portuguese funds through FCT, under Projects SAICT-PAC/0004/2015 - POCI-01-0145-FEDER-016434, POCI-01-0145-FEDER-006961, UID/EEA/50014/2013, UID/CEC/50021/2013, and UID/EMS/00151/2013, and also funding from the EU 7th Framework Programme FP7/2007-2013 under GA no. 309048.

References

[1] U.S. National Renewable Energy Laboratory, 20% Wind Energy by 2030: Increasing Wind Energy's Contribution to U.S. Electricity Supply[Online]. Available: http://www.nrel.gov/docs/fy08osti/41869.pdf.

[2] E. B. Fisher, R. P. Neill, and M. C. Ferris, "Optimal transmission switching," *Power Systems, IEEE Transactions on,* vol. 23, pp. 1346-1355, 2008.

[3] A. Nikoobakht, M. Mardaneh, J. Aghaei, V. Guerrero-Mestre, and J. Contreras, "Flexible power system operation accommodating uncertain wind power generation using transmission topology control: an improved linearised AC SCUC model," *IET Generation, Transmission & Distribution,* 2016.

[4] H. Ergun, D. Van Hertem, and R. Belmans, "Transmission system topology optimization for large-scale offshore wind integration," *IEEE Transactions on Sustainable Energy,* vol. 3, pp. 908-917, 2012.

[5] A. Nikoobakht and J. Aghaei, "IGDT-based robust optimal utilisation of wind power generation using coordinated flexibility resources," *IET Renewable Power Generation,* vol. 11, pp. 264-277, 2016.

[6] A. Khodaei and M. Shahidehpour, "Transmission switching in security-constrained unit commitment," *IEEE Transactions on Power Systems,* vol. 25, pp. 1937-1945, 2010.

[7] A. Nikoobakht, J. Aghaei, and M. Mardaneh, "Securing highly penetrated wind energy systems using linearized transmission switching mechanism," *Applied Energy,* vol. 190, pp. 1207-1220, 2017.

[8] Y. Bai, H. Zhong, Q. Xia, and C. Kang, "A Two-Level Approach to AC Optimal Transmission Switching With an Accelerating Technique," *IEEE Transactions on Power Systems,* vol. 32, pp. 1616-1625, 2017.

[9] A. Nikoobakht, J. Aghaei, and M. Mardaneh, "Managing the risk of uncertain wind power generation in flexible power systems using information gap decision theory," *Energy,* vol. 114, pp. 846-861, 2016.

[10] E. Nasrolahpour and H. Ghasemi, "A stochastic security constrained unit commitment model for reconfigurable networks with high wind power penetration," *Electric Power Systems Research,* vol. 121, pp. 341-350, 2015.

[11] A. Khodaei and M. Shahidehpour, "Transmission switching in security-constrained unit commitment," *Power Systems, IEEE Transactions on,* vol. 25, pp. 1937-1945, 2010.

[12] C. E. Murillo-Sanchez, R. D. Zimmerman, C. Lindsay Anderson, and R. J. Thomas, "Secure planning and operations of systems with stochastic sources, energy storage, and active demand," *Smart Grid, IEEE Transactions on,* vol. 4, pp. 2220-2229, 2013.

[13] H. Wu, M. Shahidehpour, A. Alabdulwahab, and A. Abusorrah, "Thermal generation flexibility with ramping costs and hourly demand response in stochastic security-constrained scheduling of variable energy sources," *Power Systems, IEEE Transactions on,* vol. 30, pp. 2955-2964, 2015.

[14] H. Wu, M. Shahidehpour, and A. Al-Abdulwahab, "Hourly demand response in day-ahead scheduling for managing the variability of renewable energy," *IET Generation, Transmission & Distribution,* vol. 7, pp. 226-234, 2013.

[15] A. Nikoobakht and J. Aghaei, "IGDT-Based Robust Optimal Utilization of Wind Power Generation Using Coordinated Flexibility Resources," *IET Renewable Power Generation,* p. 60 pp, 2016.

[16] H. Wu, M. Shahidehpour, A. Alabdulwahab, and A. Abusorrah, "Thermal Generation Flexibility With Ramping Costs and Hourly Demand Response in Stochastic Security-Constrained Scheduling of Variable Energy Sources," *Power Systems, IEEE Transactions on* vol. PP, pp. 1 - 10, 2014.

[17] F. Abbaspourtorbati, A. J. Conejo, J. Wang, and R. Cherkaoui, "Is Being Flexible Advantageous for Demands?," *IEEE Transactions on Power Systems,* vol. 32, pp. 2337-2345, 2017.

[18] M. Parvania, M. Fotuhi-Firuzabad, and M. Shahidehpour, "ISO's Optimal Strategies for Scheduling the Hourly Demand Response in Day-Ahead Markets," *Power Systems, IEEE Transactions on,* vol. 29, pp. 2636-2645, 2014.

[19] M. E. Khodayar, M. Shahidehpour, and L. Wu, "Enhancing the dispatchability of variable wind generation by coordination with pumped-storage hydro units in stochastic power systems," *IEEE Transactions on Power Systems,* vol. 28, pp. 2808-2818, 2013.

[20] M. Shahidehopour and Y. Fu, "Benders decomposition: applying Benders decomposition to power systems," *IEEE Power and Energy Magazine,* vol. 3, pp. 20-21, 2005.

[21] F. Qiu and J. Wang, "Chance-constrained transmission switching with guaranteed wind power utilization," *IEEE Transactions on Power Systems,* vol. 30, pp. 1270-1278, 2015.

[22] A. Nikoobakht and J. Aghaei, "IGDT-Based Robust Optimal Utilization of Wind Power Generation Using Coordinated Flexibility Resources," *IET Renewable Power Generation,* 2016.

[23] H. Wu, M. Shahidehpour, and A. Al-Abdulwahab, "Hourly demand response in day-ahead scheduling for managing the variability of renewable energy," *Generation, Transmission & Distribution, IET,* vol. 7, pp. 226-234, 2013.

[24] M. E. Khodayar, M. Shahidehpour, and L. Wu, "Enhancing the dispatchability of variable wind generation by coordination with pumped-storage hydro units in stochastic power systems," *Power Systems, IEEE Transactions on,* vol. 28, pp. 2808-2818, 2013.

[25] C. Sahin, M. Shahidehpour, and I. Erkmen, "Allocation of hourly reserve versus demand response for security-constrained scheduling of stochastic wind energy," *Sustainable Energy, IEEE Transactions on,* vol. 4, pp. 219-228, 2013.

[26] F. Qiu and J. Wang, "Chance-constrained transmission switching with guaranteed wind power utilization," *Power Systems, IEEE Transactions on,* vol. 30, pp. 1270-1278, 2015.

[27] A. Ahmadi-Khatir, A. J. Conejo, and R. Cherkaoui, "Multi-area energy and reserve dispatch under wind uncertainty and equipment failures," *Power Systems, IEEE Transactions on,* vol. 28, pp. 4373-4383, 2013.

[28] H. Wu, M. Shahidehpour, A. Alabdulwahab, and A. Abusorrah, "Demand response exchange in the stochastic day-ahead scheduling with variable renewable generation," *Sustainable Energy, IEEE Transactions on,* vol. 6, pp. 516-525, 2015.

[29] A. Boone, *Simulation of short-term wind speed forecast errors using a multi-variate ARMA (1, 1) time-series model*, 2005.

[30] J. Manwell, A. Rogers, G. Hayman, C. Avelar, J. McGowan, U. Abdulwahid*, et al.*, "Hybrid2–a hybrid system simulation model–theory manual," *Renewable Energy Research Laboratory, University of Massachusetts,* 2006.

[31] Q. Wang, Y. Guan, and J. Wang, "A chance-constrained two-stage stochastic program for unit commitment with uncertain wind power output," *IEEE Transactions on Power Systems,* vol. 27, pp. 206-215, 2012.

[32] M. D. McKay, R. J. Beckman, and W. J. Conover, "A comparison of three methods for selecting values of input variables in the analysis of output from a computer code," *Technometrics,* vol. 42, pp. 55-61, 2000.

[33] J. Zheng, X. Quan, Z. Jing, and Q. Wu, "Stochastic day-ahead generation scheduling with pumped-storage stations and wind power integrated," in *Probabilistic Methods Applied to Power Systems (PMAPS), 2016 International Conference on*, 2016, pp. 1-6.

[34] A. Shukla and S. Singh, "Clustering based unit commitment with wind power uncertainty," *Energy Conversion and Management,* vol. 111, pp. 89-102, 2016.

[35] G. Desrochers, M. Blanchard, and S. Sud, "A Monte-Carlo simulation method for the economic assessment of the contribution of wind energy to power systems," *IEEE Transactions on Energy Conversion,* pp. 50-56, 1986.

[36] GAMS/SCENRED.

[37] GAMS/SCENRED Documentation [Online]. Available: www.gams.com/docs/document.htm.

[38] C. Liu, J. Wang, and J. Ostrowski, "Heuristic prescreening switchable branches in optimal transmission switching," *IEEE Transactions on Power Systems,* vol. 27, pp. 2289-2290, 2012.

[39] Generalized Algebraic Modeling Systems (GAMS). [Online]. Available at http://www.gams.com.

[40] F. Bouffard, F. D. Galiana, and A. J. Conejo, "Market-clearing with stochastic security-part I: formulation," *Power Systems, IEEE Transactions on,* vol. 20, pp. 1818-1826, 2005.

[41] F. Bouffard, F. D. Galiana, and A. J. Conejo, "Market-clearing with stochastic security-part II: Case studies," *Power Systems, IEEE Transactions on,* vol. 20, pp. 1827-1835, 2005.

[42] A. Papavasiliou and S. S. Oren, “Multiarea stochastic unit commitment for high wind penetration in a transmission constrained network,” Oper. Res., vol. 61, pp. 578–592, May 2013.

[43] X. Cheng and T. J. Overbye, “PTDF-based power system equivalents,” IEEE Trans. Power Syst., vol. 20, no. 4, pp. 1868–1876, Nov. 2005.